Article

Oral Pharmacokinetics of a Chitosan-Based Nano-Drug Delivery System of Interferon Alpha

Julieta C. Imperiale[1], Inbar Schlachet[2], Marianela Lewicki[3], Alejandro Sosnik[2,*] and Mirna M. Biglione[4,*]

[1] CONICET - Universidad de Buenos Aires. Instituto de Investigaciones Farmacológicas (ININFA), Buenos Aires, Argentina; julietaimperiale@gmail.com
[2] Laboratory of Pharmaceutical Nanomaterials Science, Department of Materials Science and Engineering, Technion-Israel Institute of Technology, Technion City, Haifa, Israel; inbarschlachet@gmail.com, alesosnik@gmail.com
[3] CONICET - Universidad de Buenos Aires. Instituto de Investigaciones en Microbiología y Parasitología Médica (IMPAM); vetmarianelalewicki@gmail.com
[4] CONICET - Universidad de Buenos Aires. Instituto de Investigaciones Biomédicas en Retrovirus y Sida (INBIRS), Buenos Aires, Argentina; mbiglione@fmed.uba.ar
* Correspondence: mbiglione@fmed.uba.ar (M.B.), sosnik@technion.ac.il (A.S.)

Abstract: Interferon alpha (IFNα) is a protein drug used to treat viral infections and cancer diseases. Due to its poor stability in the gastrointestinal tract, only parenteral administration ensures bioavailability, which is associated with severe side effects. We hypothesized that the nanoencapsulation of IFNα within nanoparticles of the mucoadhesive polysaccharide chitosan would improve the oral bioavailability of this drug. In this work, we produced IFNα-loaded chitosan nanoparticles by the ionotropic gelation method. Their size, size distribution and concentration were characterized by dynamic light scattering and nanoparticle tracking analysis. After confirming their good cell compatibility in Caco-2 and WISH cells, the permeability of unmodified and PEGylated nanoparticles was measured in monoculture (Caco-2) and co-culture (Caco-2/HT29-MTX) cell monolayers. Results indicated that the nanoparticles cross the intestinal epithelium mainly by the paracellular route. Finally, the oral pharmacokinetics in BalbC mice of nanoencapsulated IFNα revealed that it was absorbed reaching an area-under-the-curve of 56.9 pg.h/mL.

Keywords: IFNα; polymeric nanoparticles; oral protein delivery; in vitro intestinal permeability; oral pharmacokinetics.

1. Introduction

Biological drugs are increasingly positioned in the pharmaceutical market because their high affinity for the different therapeutic targets enhances treatment efficacy and lowers side-effects. However, their high molecular weight, low lipophilicity and polyelectrolyte nature preclude absorption by transmucosal routes that are more patient compliant. Besides, in the case of oral administration, they are exposed to hydrolytic and enzymatic degradation conditions along the gastrointestinal tract (GIT) that compromise their oral bioavailability (1).

Interferon alpha (IFNα) is a cytokine that exhibits a broad spectrum of antiviral, immunomodulatory, antiproliferative and antitumoral activities that supports its therapeutic potential (2). IFNα stimulates the innate-immune response and directs the transition from innate to acquired immunity and induces the differentiation of monocytes into dendritic cells (3), which are antigen-presenting cells. In addition, the antitumor and antiviral activity of IFNα stems from the activation of CD4+ and CD8+ T lymphocytes and natural killer cells, by increasing their cytotoxic activity and their ability to produce IFN gamma (IFNγ) that in turn enhances the secretion of other

cytokines (4,5). Furthermore, IFNα upregulates the expression of tumor-associated surface antigens and major histocompatibility complex (MHC) class I antigens that improve antigen recognition, induces pro-apoptotic genes and proteins, suppress anti-apoptotic genes, modulates cell-differentiation, and inhibits angiogenesis that is a key stage in tumor growth and metastasis (3). All these mechanisms contribute to its activity against malignant cells. IFNα has been approved in the treatment of different types of cancer, including hairy cell leukemia, malignant melanoma, acquired immunodeficiency syndrome-related Kaposi's sarcoma, follicular non-Hodgkin's lymphoma and condyloma acuminate (6), and chronic viral infections such as hepatitis B and C (6). To treat these diseases, IFNα is daily administered by subcutaneous or intramuscular injection, which is associated with strong pain and poor patient compliance. In addition, the half-life of IFNα is very short, e.g., 2.2 and 2.9 h after intramuscular and subcutaneous administration, respectively (7). Commercial formulations of PEGylated IFNα (e.g., Pegasys® and PegIntron®) prolong the half-life of IFNα in the systemic circulation enabling a weekly administration although it implies a significant activity loss of 80% with respect to the non-PEGylated form (8). The investigation of new IFNα formulations with a better benefit-risk ratio is called for. Polymeric-based nanoparticulate systems are able to load therapeutic proteins maintaining its conformational structure and stability, so retaining the biological activity of the protein (9,10). Furthermore, polymeric carriers protect the cargo from chemical and/or enzymatic degradation (9). They can effectively cross the intestinal membrane depending on the size, shape, surface area, charge of the carrier, as well as the hydrophobicity and hydrophilicity of the polymer and their functional groups (9). Most of studies in the field of polymeric-based particulate systems for oral delivery of therapeutic proteins have been focused on the encapsulation of insulin (11–14). Due to the promising results obtained, the advance towards other proteins is of interest. In this context, we previously developed recombinant IFNα-loaded chitosan (CT) nanoparticles (IFN-CT-NPs) to achieve the absorption of the drug in the gastrointestinal tract. Remarkably, this carrier did not jeopardize the biological activity of the protein and enables its oral absorption in CF1 mice (15). This was assessed in a preliminary study involving the analysis of only one detection time point that was taken as a rapid indicator of absorption. However, not only a better understanding of the pathways involved in the absorption process is of relevance but also a thorough pharmacokinetic study is needed to approach an appropriate drug regimen for eventually achieve its translation from bench to bedside. Accordingly,
in this work, we produced IFN-CT-NPs by the ionotropic gelation method and fully characterized the nanoparticle size, size distribution and concentration by dynamic light scattering (DLS) and nanoparticle tracking analysis (NTA). Then, the cell compatibility of the nanoparticles was assessed in Caco-2 (a model of intestinal epithelium) and WISH cells (a human amnion-derived cell line) and the permeability of unmodified and PEGylated nanoparticles was measured in monoculture (Caco-2) and co-culture (Caco-2/HT29-MTX) cell monolayers. Finally, the oral pharmacokinetics of nanoencapsulated IFNα was studied in BalbC mice. Overall results highlight the promise of this novel nanoformulation for the safe and effective oral administration of this key biological drug.

2. Materials and Methods

2.1. Materials

CT (GC9009, batch 769FGD, molecular weight of ~50,000 g/mol, degree of deacetylation of ~94% and viscosity of ≤100 mPa.s) was purchased from Glentham Life Sciences (Corsham, UK). The degree of deacetylation measured in our laboratory by proton nuclear magnetic resonance (1H-NMR, 400-MHz Bruker® Avance III High Resolution spectrometer, Bruker BioSpin GmbH, Rheinstetten, Germany with SpinWorks 4.0 software, University of Manitoba, Canada) using 5% w/v solution was prepared in deuterium oxide (D2O, Sigma-Aldrich) and 142 trifluoroacetic acid (5% v/v, Sigma-Aldrich) was 94.5% (16,17) and the number- and weight-molecular weight were 53,000 and 79,000 g/mol, respectively, as determined by gel permeation chromatography (17). Sodium tripolyphosphate pentabasic (TPP) were supplied by Sigma-Aldrich (USA). Acetic acid was purchased from Merck Chemicals GmbH (Germany) and IFNα-2b (BIOFERON®, lyophilized powder) from BioSidus (Argentina). PEG-

carboxymethyl (mPEG5000-COOH, molecular weight of 5000 g.mol-1) was supplied by Laysan Bio, Inc. (USA).

2.2. Preparation of IFNα-loaded nanoparticles

Blank and IFNα-loaded CT-NPs were prepared by the ionotropic gelation method between the polycationic CT and TPP anions as described before resulting in NPs with a positive surface, of +30 mV, with conserved bioactivity (15). To assess the effect of PEGylation on the permeability of CT-NPs, we prepared PEG.CT-NPs by using a mixture of pristine CT and PEGylated CT (PEG.CT) in a 1:1 weight ratio. CT was PEGylated by a two-step covalent coupling protocol reported by Chang et al. (18). Briefly, mPEG5000-COOH (50 mg) was added to a solution of N-hydroxy succinimide (288 mg, NHS, 5 mM, Thermo Fisher Scientific, USA), 1-ethyl-3-(3-dimethylaminopropyl)carbodiimide hydrochloride (191.7 mg, EDC, Thermo Fisher Scientific) in 2-(N-morpholino) ethanesulfonic acid buffer (MES, 0.05M, 5 mL, Molekula, USA). The solution was kept under constant magnetic stirring at room temperature for 15 min. Then, activated mPEG5000-COOH was reacted with the primary amine moities of CT in solution (2 mg/mL, 125 mL) dissolved in acetic acid (0.33% v/v). The product was dialyzed for 72 h and lyophilized (Labconco Free Zone 4.5 plus L Benchtop Freeze Dry System, USA). PEG.CT was characterized by Fourier transform infrared (FTIR) spectroscopy using an Equinox 55 spectrometer (Bruker Optics Inc., Germany) and KBr disks (Merck KGaA, Germany). The scanning range was 4000 to 400 cm−1, 32–64 scans and a resolution of 4 cm−1. In addition, it was analyzed by proton-nuclear magnetic resonance spectroscopy (1H-NMR, 400 MHz Bruker® Avance III High Resolution Spectrometer) using dimethyl sulfoxide-d6 (DMSO-d6, Sigma-Aldrich) as solvent. Chemical shifts are reported in ppm using the peak of DMSO at 2.50 ppm as internal standard. The weight content of mPEG5000 in CT was estimated by interpolation in a calibration curve built from physical mixtures of CT and mPEG5000-COOH in acetic acid-d4 using different CT:mPEG weight ratios between 0.02 and 0.7. Characteristic signals of each compound in the physical mixtures, namely 2.8 ppm (HC-NH2) of CT and 3.3 ppm (CH3O) of mPEG5000-COOH were used for the integration (R2 = 0.9766).

2.3. Characterization of the nanoparticles

2.3.1. Particle size, size distribution and zeta-potential.

The particle size (hydrodynamic diameter, Dh) and size distribution (polydispersity index, PDI) of the unloaded and IFNα-loaded NPs were measured by DLS (Zetasizer Nano-ZS, Malvern Instruments, UK), provided with a He–Ne (633 nm) laser and a digital correlator ZEN3600 using an angle of θ = 173° to the incident beam, at 25°C. Results are expressed as number-based distribution of three samples prepared under identical conditions and each one of them is the result of at least four runs.

2.3.2. Nanoparticle tracking analysis.

The quantification of the NP concentration (particles per mL of suspension) and the visualization of their Brownian motion was carried out by NTA (NanoSight® NS500-Zeta HSB system with a high sensitivity camera and 638 nm laser for fluorescence analysis, Malvern Instruments) under scattering mode.

2.3.3. Stability of nanoparticles as a function of pH.

A sample of fresh NPs was placed for 15 min in a solution of pH ranged from 1 to 8 (1:5 volume ratio of NPs:medium). Then, the Dh was measured by DLS as was described before.

2.4. Cell studies in vitro

2.4.1. Cells.

The human epithelial adherent cell line WISH was kindly donated by Prof. José Luis López from the Department of Virology (Faculty of Pharmacy and Biochemistry, University of Buenos Aires, Argentina). Cells were cultured in Eagle's Minimum Essential Medium (EMEM, Life Technologies

Corp., USA) supplemented with 10% heat-inactivated fetal bovine serum (Internegocios, Argentina), penicillin, L-glutamine and no essential amino acids (Sigma-Aldrich). Cells were maintained at 37°C in humidified air with 5% of CO2. Cells were collected every 3-4 days (TrypLE Express enzyme, Gibco, USA) and the number of living cells were quantified by the trypan blue exclusion assay 0.4% (Sigma-Aldrich). The human epithelial cell line Caco-2 (HTB-37TM) was supplied by ATCC® (USA) and the mucus-secreting HT29-MTX cell line was purchased from Sigma-Aldrich. These cells were cultured in Dulbecco's Modified Eagle's Medium (DMEM, Life Technologies Corp.) supplemented with L-glutamine, 10% heat-inactivated fetal bovine serum (FBS, Sigma-Aldrich) and penicillin/streptomycin (5 mL of a commercial mixture of 100 U per mL penicillin + 100 µg per mL streptomycin per 500 mL medium, Sigma-Aldrich), maintained at 37°C in a humidified 5% CO2 atmosphere and split every 4–5 days.

2.4.2. Cell compatibility and permeability assays.

The cell compatibility of CT-NPs and PEG.CT-NPs was evaluated in the Caco-2 cell line. For this, cells were cultured on 96-well plates at a density of 2.5 x 104 cells/well for 24 h to reach confluence. Then, the cell medium was replaced by a mixture of fresh medium cell (100 µL) and a dilution (100 µL) of CT-NPs or PEG.CT-NPs in cell medium. All NPs were previously sterilized by filtration (MF-Millipore TM 0.22 µm, Merck Millipore, Germany). Cells were exposed to the NP suspensions for 24 h, the medium was removed, and new medium (100 µL) and sterile 3-(4,5-dimethylthiazol-2-yl)-2,5-diphenyltetrazolium bromide solution (MTT, 25 µL, 5 mg/mL, Sigma-Aldrich) was added. Cells were incubated for 4 h at 37 °C under 5% CO2 atmosphere, the medium was removed, formazan crystals dissolved with DMSO (Sigma-Aldrich) and quantified spectrophotometrically at 530 nm with reference at 670 nm (Multiskan GO, Thermo Fisher Scientific Oy, Finland). Cell cultured in medium without NPs were used as control (100% viability). The cell compatibility of the NPs selected to be orally administered to mice was also assessed in WISH cells. For this, cells were seeded onto 96-well plates at a density of 2.5 x 104 cells/well and allowed to grow for 24 h to reach confluence. Then, the cell medium was replaced by a mixture of fresh medium (100 µL) and a dilution (100 µL) of (i) blank CT-NPs, (ii) IFN-CT-NPs, (iii) CT solution and (iv) free IFNα solution in cell medium. All specimens were previously sterilized by filtration (MF-MilliporeTM Membrane Filter, 0.22 µm pore size, Merck KGaA, Germany). Cells were exposed to each treatment for 24 h. Then, the supernatant was withdrawn and the commercial reactive CellTiter 96® AQueous One Solution (Promega, USA) containing 3-(4,5-dimethylthiazol-2-yl)-5-(3-carboxymethoxyphenyl)-2-(4-sulfophenyl)-2H-tetrazolium (MTS) was added. Cells were incubated for 20 min and the absorbance was measured at 492 nm using a microplate spectrophotometer (Multiskan GO). The percentage of viability was calculated by extrapolation from a calibration curve prepared with growing amounts of WISH cells (0.25, 0.5, 1.0, 1.5, 2.0 and 2.5 x 104 cells/well) incubated only with culture medium.

For permeability studies, in a monoculture model, Caco-2 cells (3 × 105 cells per well) were seeded in cell culture inserts (ThinCert™, culture surface of 113.1 mm2, 3.0 µm pore size, Greiner Bio-One GmbH, Germany) maintained in 12-well plates (15.85 mm diameter, 16.25 mm height, Greiner CELLSTAR) with 0.5 and 1.5 mL of DMEM medium in the donor (apical) and acceptor (basolateral) chambers, respectively. Cells were incubated 10-25 days, the culture medium was replaced every 2–3 days and the integrity of the cell monolayer was characterized by trans-epithelial electrical resistance (TEER) measurements performed with an epithelial volt-ohm-meter (“EVOM2”, WPI, USA). For permeability experiments, only inserts where the resistance was higher than 260 Ω cm2 were used. Permeability experiments were also performed in co-culture monolayers of Caco-2:HT29-MTX (9:1 number ratio). For this, the same cell density was seeded and the protocol carried out as described above. The test sample consisted of a stock dispersion of blank CT-NPs and PEG.CT-NPs fluorescently-labeled with fluorescein thioisocyanate (FITC, Sigma-Aldrich) and diluted with transport medium. For preparation of FITC-labeled CT that was then mixed with PEG.CT to produce fluorescently-labeled PEGylated NPs, a synthetic method described elsewhere with a little modification was used (19). Briefly, 20 mL of methanol was added to 20 mL of 1% w/v CT in a 0.05 M nitric acid solution. Then, 20 mL of a solution of FITC previously dissolved in methanol (2 mg/mL) was added under magnetic stirring. The reaction was allowed to proceed for 3 h at room temperature and protected from light. The

resulting solution was purified by dialysis (nominal MWCO of 3500 Da, Cellu Sup® T1 nominal flat width of 46 mm, diameter of 29.3 mm, and volume/length ratio of 6.74 mL/cm; Membrane filtration products, Inc., USA) for 72 h and lyophilized. To produce FITC-labeled NPs, a mixture of unlabeled and fluorescently-labeled CT (weight ratio of 1:1) was used as described above. Immediately before the beginning of the experiment, the cell culture medium was replaced by Hank's Balanced Salt Solution (transport medium, HBSS, Sigma-Aldrich) buffered to pH 6.8 with 25 mM of 4-(2-hydroxyethyl)-1-piperazineethanesulfonic acid (HEPES, Sigma-Aldrich) to a final concentration of 720 μg/mL in both the donor (apical, 0.45 mL) and the acceptor (basolateral, 1.2 mL) chambers. After 5, 10, 15, 30, 60, 90, 120, 180 and 240 min, 600 μL was extracted from each acceptor chamber to quantify the concentration of NPs that crossed the cell monolayer by fluorescence spectrophotometry (Fluoroskan Ascent Plate Reader, Thermo Fisher Scientific Oy) utilizing black 96-well flat bottom plates (Greiner Bio-One, Austria) at wavelengths of 355 nm for excitation and 635 nm for emission. The apparent permeability coefficient (Papp) was calculated according to Equation 1

$$Papp = dc/dt \times 1/(A \times Co) \qquad (1)$$

Where dc/dt is the transport rate (μg.s−1) across the monolayer, Co is the initial concentration of NPs in the donor compartment (μg.cm−3) and A is the surface area of the membrane (cm2).

2.4.3. Cell uptake.

To gain further insight into the cell uptake of the NPs, the permeability test in the co-culture of Caco-2:HT29-MTX (9:1 number ratio) was continued for 24 h. Then, cells were harvested by trypsinization (trypsin-EDTA 0.25%, Sigma-Aldrich), washed with fresh medium to remove non-internalized NPs and transferred to a 96-well plate with trypan blue (0.4% w/v, 50 μL, Sigma-Aldrich) to quench the fluorescence of the NPs adhered to the cell surface. As control of quenching, the fluorescence of a dilution of FITC-labeled NPs (without cells) with trypan blue was quantified.

2.5. Oral pharmacokinetics

The oral bioavailability was assessed in female BALB/c mice aged 8-10 weeks purchased from the National University of La Plata (Argentina). The preclinical protocol was approved by the Institutional Committee for the Care and Use of Experimental Animals (CICUAL) of the Faculty of Medicine (Resolution #2609/2016, University of Buenos Aires, Argentina). Animals were fasted for 2 h prior the administration. Then, IFN-CT-NPs (400 μL, 0.3 MIU) were orally administered by gavage using a straight stainless steel probe (n = 20). The dose was selected based on the recommended dose for most therapies (5 MIU/m2) adjusted to the average body surface of each mouse. The value obtained was multiplied arbitrarily by 10 given that it is known that the oral bioavailability is lower than the parenteral one. Three samples were extracted from each mouse. The first two by sub-mandibular puncture, and the last one by cardiac puncture, after intraperitoneal administration of anesthesia (ketamine 150 mg/kg and xylazine 10 mg/kg, Sigma-Aldrich). Altogether, samples were obtained at the following time points post-administration: 15, 30, 45, 60, 120, 150, 180, 240, 300 and 360 min. As control, blood samples were obtained from mice (n = 2) by cardiac puncture at 30 min post-administration of the following treatments: (i) water, (ii) free IFNα, (iii) a mixture of IFNα and a CT solution and (iv) a mixture of free IFNα and blank CT-NPs. Samples were centrifuged to separate cells and plasma was frozen at -80°C until analysis. Plasma IFNα levels were quantified by ELISA according the instructions of the manufacturer (Affimetrix, EBiosciences, Austria). The following pharmacokinetic parameters were calculated using a non-compartmental model (TOPFIT program version 2.0, Dr. Karl Thomae Gmbh, Schering AG, Germany): (i) maximum plasma concentration (Cmax), (ii) time to Cmax (tmax) and (iii) the area-under-the-curve between 0 and ∞ (AUC0-∞).

2.6. Statistical analysis

Statistical analysis was performed by t-test or one-way analysis of variance (ANOVA, significance level of 5%) with Bonferroni test using Graph Pad Prism version 7 for Windows.

3. Results and discussions

3.1. Synthesis and characterization of PEGylated chitosan

Aiming to compare the mucoadhesiveness and the mucopenetration of CT-NPs in a model of intestinal epithelium in vitro, we synthesized PEG.CT-NPs. This modification relies on the ability of PEG to minimize the interaction between CT and mucus (20). For this, CT was primarily PEGylated by the condensation of the terminal carboxylate group of mPEG5000-COOH with the amine groups in the side-chain of CT utilizing the EDC/NHS chemistry (18). The successful synthesis was confirmed by FTIR and 1H-NMR (Supplementary **Figure S1**). The FTIR spectrum showed the typical absorption bands of pristine CT at 3448 cm-1 corresponding to the overlapping of O-H and N H stretching, at 2900 cm-1 due to CH2 groups, at 1670 cm-1 owing to the C=O stretching of the remaining amide, at 1617 cm-1 a weak band due to N-H bending of amine and at 1087 cm-1 owing to the C-O stretching of ether (Supplementary **Figure S1A**). Conversely, the spectrum of PEG.CT showed the characteristic bands of CT together with an increase in the intensity of the peak at 1087 cm-1, which corresponds to the stretching vibrations of C-O-C bond, the main characteristic absorption band of PEG. Furthermore, a new strong band at 1560 cm-1 was consistent with the conjugation of PEG blocks to the CT side-chain through the formation of amide moieties. In addition, appearance of a new peak at 3.3 ppm in the 1H-NMR spectrum of PEG-CT confirmed the PEGylation (Supplementary **Figure S1B**). This method was also utilized to quantify the PEG content in the product by utilizing a calibration curve built with CT/mPEG5000 physical mixtures with different weight ratios and it was 12.6% w/w.

3.2. Preparation and characterization of the nanoparticles

CT-NPs showed one single size population with Dh of 47 nm and PDI of 0.47, as determined by DLS (**Table 1**). PEGylation led to a sharp size growth to 93 nm (PDI = 0.32), due to the formation of a highly hydrated corona of PEG blocks (**Table 1**). In addition, the NP concentration was quantified by NTA. Pristine (1.6 mg/mL) and PEGylated NPs (1.75 mg/mL) showed concentrations of 3 x 1011 ± 6 x 107 and 3 x 1011 ± 3 x 1010, respectively (**Table 1**); the concentration of the NPs was adjusted to ensure identical CT concentration in both samples.

Table 1. Hydrodynamic diameter (Dh), polydispersity index (PDI) and concentration of CT-NPs and PEG.CT-NPs, as measured by DLS and NTA.

Parameter	CT-NPs	PEG.CT-NPs
D_h (nm)	47.0	93.0
PDI	0.47	0.32
Concentration (particles/mL)	$3 \times 10^{11} \pm 6 \times 10^{7}$	$3 \times 10^{11} \pm 3 \times 10^{10}$

3.3. Cell compatibility, permeability and uptake

CT has a known safety profile by the oral route, it is classified as a "generally recognized as safe" ingredient by the Food and Drug Administration (FDA) and approved as food supplement in Japan, Italy, Finland and Brazil. CT is commercialized as ChitoClear® by Primex to bind fatty acids and prevent their oral absorption (21). In addition, the good cell compatibility of different types of CT-NPs, including amphiphilic ones, was reported elsewhere (22). As a preamble to the permeability

and uptake studies, the Caco-2 cell compatibility of CT-NPs and PEG.CT-NPs was assessed under the same conditions (time and concentration) used in the permeability assays. Both types of NPs showed approximately 100% viability (**Figure 1A**). Then, their permeability across a monolayer of Caco-2 cells was evaluated in order to learn whether PEGylation modifies the permeability or not. Caco-2 is a human epithelial cell line widely used as a model of the intestinal epithelial barrier (23). Results showed that 19.4 ± 2.6% of PEG.CT-NPs and 21.1 ± 4.8% of CT-NPs crossed the Caco-2 monolayer after 4 h (**Figure 1B**). In addition, both curves displayed almost identical slope and, as expected, similar Papp values; 5.531 x 10-6 ± 6.504 x 10-7 and 6.064 x 10-6 ± 1.162 x 10-6 cm/s for PEGylated and unmodified NPs, respectively, with no significant differences. These values suggest that these nanocarriers have a moderate permeability (24).

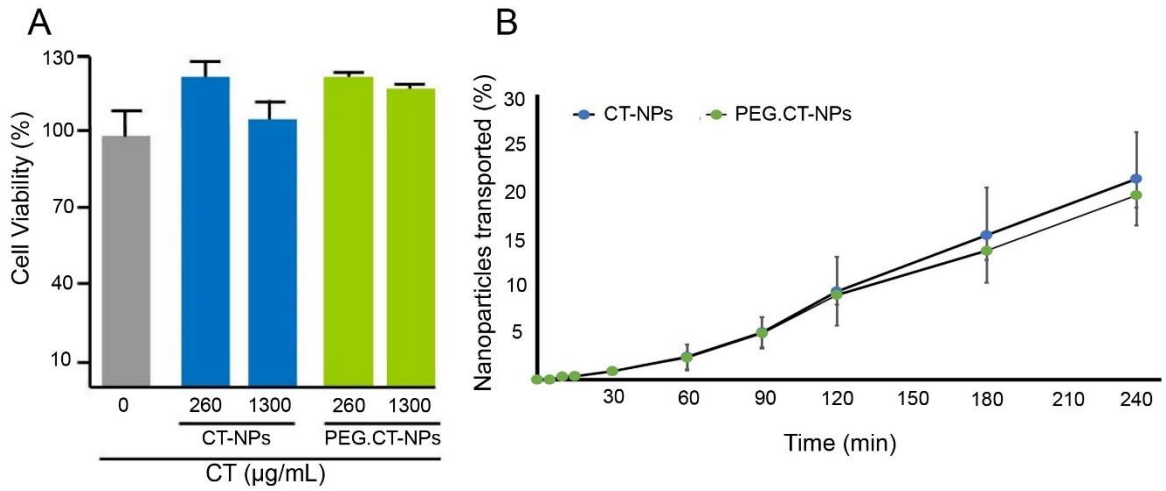

Figure 1. (A) Caco-2 cell viability upon exposure to different concentrations of CT-NPs and PEG.CT-NPs, as determined by the MTT assay and (B) Cumulative transport of CT-NPs and PEG.CT-NPs across Caco-2 cell monolayers. Values are expressed as the mean ± S.D.

However, monoculture of Caco-2 monolayers is a simplified model of the intestinal epithelium. To more closely simulate the physiological conditions, a co-culture of Caco-2:HT29-MTX (9:1) cells was used; HT29-MTX are mucin-secreting cells. This model enabled to study the effect of PEGylation on the interaction of the NPs with mucus and the contribution of mucin to the permeability of the nanoparticles. Results showed that 16.0 ± 0.3% (Papp = 4.486 x 10-6 ± 8.691 x 10-8 cm/s) and 22.6 ± 3.9% (Papp = 7.006 x 10-6 ± 1.050 x 10-6 cm/s) of PEG.CT-NPs and CT-NPs permeated after 4 h, respectively (**Figure 2A**). These results indicated that the presence of mucin does not affect the permeability of pristine CT-NPs. Conversely, a significant decrease in the Papp was observed for PEG.CT-NPs ($p < 0.05$) (**Figure 2B**). This behavior could be explained by two possible phenomena: (i) the formation of entanglements between PEG blocks and mucin that prevents NPs from reaching the apical surface of the epithelial cells and (ii) a decrease in the concentration of the free amine groups of CT that are involved in the opening of epithelial tight junctions. Based on these results, CT-NPs were selected to conduct further permeability studies.

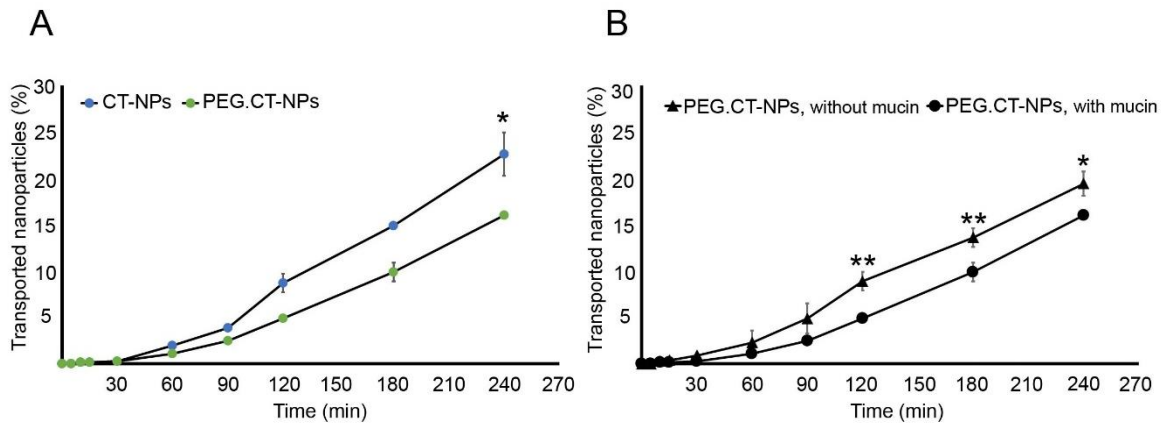

Figure 2. Cumulative transport of (A) CT-NPs and PEG.CT-NPs across a co-culture of Caco-2 cells:HT29 (9:1) and (B) PEG.CT-NPs across a monolayer of Caco-2 cells and a co-culture of Caco-2HT29 (9:1) cells. Values are expressed as the mean ± S.D. (n=3).

Aiming to gain insight into the transport mechanisms involved in the permeability of CT-NPs across a co-culture Caco-2/HT29-MTX cell monolayer, the study was continued for 24 h. Findings confirmed that 41.0 ± 8.0% of the initial amount of NPs permeated the monolayer detecting them in the acceptor chamber, while 45.7 ± 5.5% of the nanoparticles remained in the donor chamber. The difference to complete 100% of the initial amount of CT-NPs (13.3%) probably interacted with the cell monolayer by adsorption on the cell surface or cellular uptake (22). To investigate if this percentage was internalized or only adhered to cell surface, we trypsinized and washed the cells and quantified the fluorescence with and without the addition of trypan blue which is a dye that quenches external, though not internal fluorescence because it is unable to penetrate intact cell membranes. Before the addition of trypan blue, 7.6 ± 2.7% of CT-NPs were quantified from the cell suspension, a value that was quite similar to the theoretical value of 13.3%. Conversely, when the fluorescence was determined after the addition of trypan blue, values were undetectable. These results strongly suggested that CT-NPs are not endocytosed by enterocytes and that the NPs retained by the cell monolayer are mainly adsorbed onto the cell surface by electrostatic interactions between the positively-charged CT and the negatively-charged membrane. Although the in vitro model used in this work does not rule out the transport of CT-NPs through M cells (not represented in the co-culture of), our results are in line with transport by a paracellular transport.

Finally, since the cell compatibility depends not only on the NP properties (e.g., composition and size) but also on the cell type, we also evaluated the compatibility of CT-NPs in the line of human epithelial cells WISH. Results showed that there were no significant differences in the viability of the WISH cells treated with CT-NPs (2-20000 ng/mL CT) and the control (**Figure 3**). Equivalent doses of CT in solution did not show toxic effects.

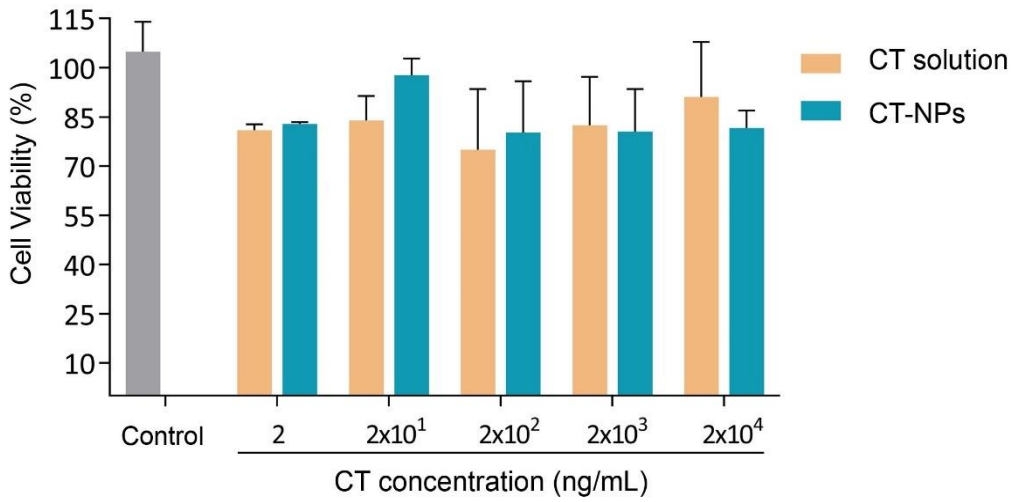

Figure 3. WISH cell viability upon exposure to different concentrations of CT solution and CT-NPs. Values are expressed as the mean ± S.D. (n = 3).

The physical stability of CT-NPs was determined under physiologically relevant pH conditions. Results showed that CT-NPs were stable in both, acid and neutral pH mediums (**Figure 4**). A 4-fold size increment was observed at pH 7.5 as was expected. Therefore, this nano-drug delivery system could pass through the gastrointestinal tract without undergoing major changes in its structure due to pH.

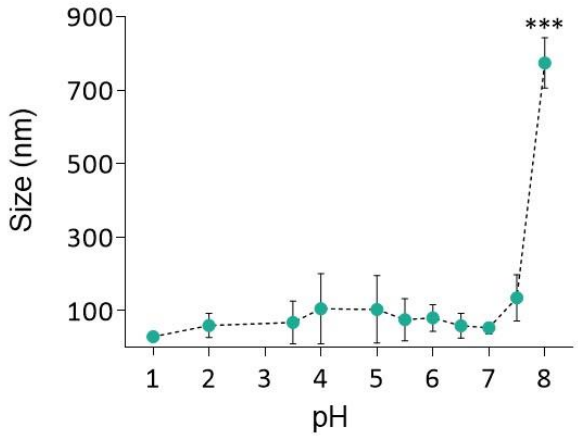

Figure 4. Stability of CT-NPs under different conditions of pH.

3.4. Oral pharmacokinetics

In a preliminary pharmacokinetic study, we showed that IFNα is detected in the systemic circulation 1 h after the oral administration of IFN-CT-NPs to CF1 mice (15). Contrariwise, at this time point, free IFNα could not be detected (15), in full agreement with studies conducted in mice, rabbits, dogs and monkeys (25). Remarkably, our previous results were the first to show the oral absorption of the biological drug. However, these studies were conducted utilizing outbred mice that usually result in greater data variability. In addition, a complete pharmacokinetic study is needed to understand the absorption and elimination pathways. Thus, in this work, we used an inbred strain, female BALC/c mice. As shown in **Figure 5A**, after oral administration of a single dose of 0.3 MIU of IFN-CT-NPs, the concentration of IFNα in plasma showed two maxima peaks. The first at 0.5 h (Cmax = 48.4 ± 22.5 pg/mL) and the second one at 1.5 h (27.6 ± 31.4 pg/mL). In addition, the levels of IFNα in plasma were undetectable 3 h after administration. To absorption peaks are typically associated with an enterohepatic recirculation phenomenon, though IFNα is a highly labile protein and recirculation is

unlikely. In this context, the first peak would correspond to primary conventional intestinal absorption, while the second at a later time to lymphatic absorption that is slower than the intestinal one. It is important to stress that particles with sizes <3 μm can translocate to the gut-associated lymphoid tissue (GALT) migrating into the mesenteric lymph nodes and appearing in the lymph between 10 min and 3 h after administration, as a function of nutritional conditions and particle size (26). Other possibility would involve the absorption of the drug in two different portions of the gut. The AUC0-∞ obtained was 56.9 pg*h/mL, which is a promising result considering that a pharmacokinetic study involving healthy volunteers showed that the Cmax and AUC were of 853 pg/mL and 994 pg*h/mL, respectively, after the intravenous administration of IFNα-2b (5 MIU), and of 207.9 pg/mL and 2850 pg*h/mL, respectively, after the subcutaneous administration of the drug (5 MIU) (7). Consequently, considering the dose adjustment, the values obtained in this study are in good agreement with those obtained in human volunteers. Similarly, the Cmax and AUC obtained after a single subcutaneous injection of the drug (3 MIU) to patients with chronic hepatitis C virus infection were 42 pg/mL and 879 pg*h/mL, respectively (27).

As control, we confirmed that after the oral administration of free IFNα, PEGylated IFNα and free IFNα co-administered with either blank CT-NPs or a CT solution, IFNα could not detected at 0.5 h (the first maximum absorption time) (**Figure 5B**). Outstandingly, the concentration of IFNα detected in plasma after the subcutaneous administration of free IFNα (46.7 ± 38.3 pg/mL) was similar to the obtained with the oral administration of IFN-CT NPs (48.4 ± 22.5 pg/mL) after 2.5 h. These results highlight the potential of this nanocarrier for the improved oral delivery of this biological drug.

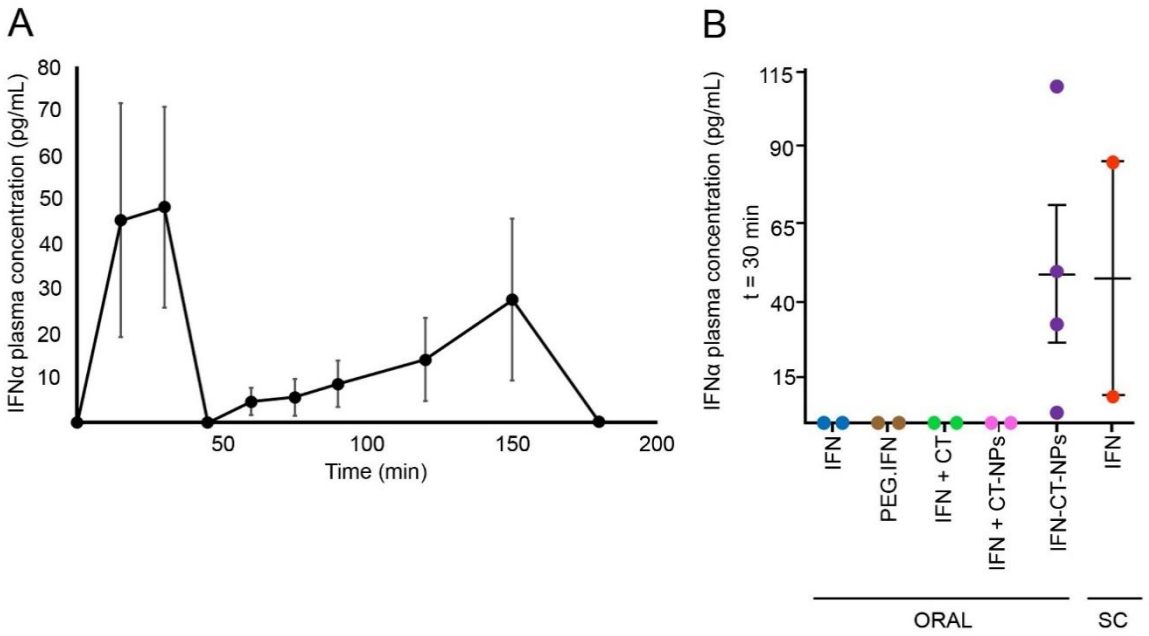

Figure 5. Oral pharmacokinetics of IFNα. (A) Mean plasma concentration (± S.E.M.) – time profile of IFNα after oral administration of IFN-CT-NPs (dose = 0.3 MIU) to BALB/c mice and (B) IFNα plasma concentration (± S.E.M) in mice at 0.5 h after the orally administration of commercial free IFNα (IFN), commercial PEGylated-IFNα (PEG-IFN), a physical mixture of free IFNα and blank CT-NPs (IFN + CT-NPs), a physical mixture of free IFNα and a CT solution (IFN + CT) or IFN-CT NPs. An additional group was subcutaneously treated with commercial free IFNα.

4. Conclusions

In this work, we produced CT-NPs and PEG.CT-NPs as a nanotechnology platform for the encapsulation and oral administration of IFNα. After the characterization of the nanoparticles, we studied their cell compatibility and permeability in vitro. These nanocarriers exhibited a moderate permeability across a co-culture Caco-2/HT29-MTX cell monolayer mainly by the paracellular

pathway. PEGylation of the nanoparticles did not improve permeability and was detrimental most probably due to the formation of entanglements with mucin or the more limited ability of the nanoparticles to open epithelial tight junctions. Finally, we investigated for the first time the oral pharmacokinetic profile of this popular biological drug. Oral administration of IFN-CT-NPs led to a bioavailability of 56.9 pg/mL*h in BAL/c mice. The concentration of IFNα detected in plasma after the oral administration of IFN-CT-NPs was similar to the obtained by subcutaneous administration of free IFNα. These data highlight the potential of this nano-drug delivery system for the oral administration of this popular biological drug. Future studies will investigate the efficacy of this nanoformulation in animal models of diseases that are treated with IFNα as first-line medication.

Author Contributions: Contributions were distributed as follows: conceptualization, J.C.I., M.M.B. and A.S.; methodology, J.C.I., I.S. and M.L.; writing—original draft preparation, J.C.I.; writing—review, A.S. and M.M.B.

Funding: This work was supported by the National Agency for Scientific and Technological Promotion (PICT N° 2012-0322) and the National Scientific and Technical Research Council (PIP N° 112 20110100644). Also, this research received partial support by the Russell Berrie Nanotechnology Institute (RBNI, Technion).

Acknowledgments: JCI and MB are researchers of CONICET. AS is correspondent researcher of CONICET. We thank Dr. Camila Cánepa for technical support in the development of CT-NPs, Prof. Paul Fisch (Institute of Clinical Pathology, University of Freiburg, Germany) for providing the ELISA kit for IFNα quantification, Dr. Cristian Hocht (Department of Pharmacology, University of Buenos Aires, Argentina) for technical support in the pharmacokinetics analysis and Dr. Magdalena Gherardi (Instituto de Investigaciones Biomédicas en Retrovirus y Sida, Argentina) for their precious assistance in the in vivo experiments.

Conflicts of Interest: The authors declare no conflict of interest.

Appendix A

Supplementary Materials:

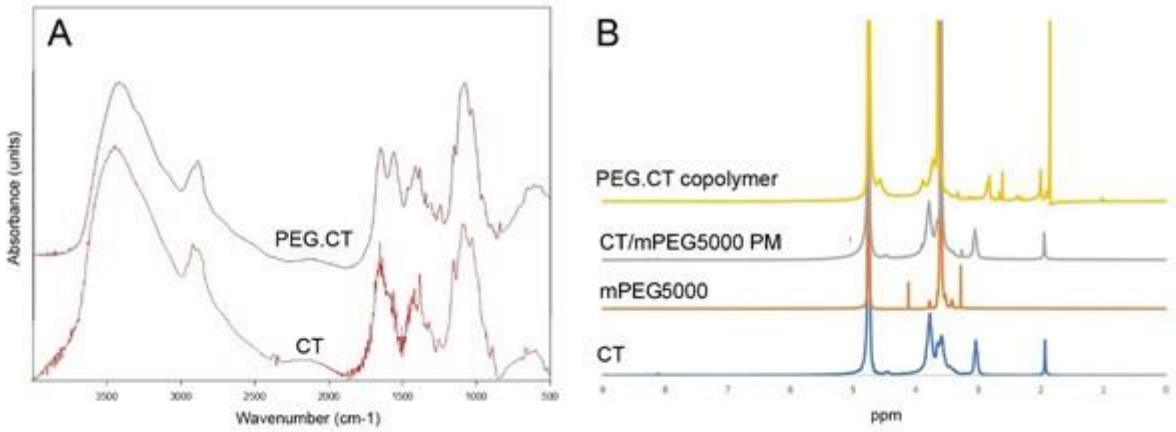

Supplementary Figure S1. Characterization of PEG.CT. (A) FTIR spectra of CT and PEG.CT and (B) 1H-NMR spectra of CT, mPEG5000, a physical mixture (PM) of mPEG and CT and PEG.CT.

References

1. Liu C, Kou Y, Zhang X, Cheng H, Chen X, Mao S. Strategies and industrial perspectives to improve oral absorption of biological macromolecules. Expert Opin Drug Deliv [Internet]. 2018;15(0):223–33. Available from: http://dx.doi.org/10.1080/17425247.2017.1395853

2. Katze MG, He Y, Gale M. Viruses and interferon: a fight for supremacy. Nat Rev Immunol [Internet]. 2002 Sep [cited 2019 Jun 3];2(9):675–87. Available from: http://www.nature.com/articles/nri888

3. El-Baky NA, Redwan EM. Therapeutic Alpha-Interferons Protein: Structure, Production, and Biosimilar. Prep Biochem Biotechnol [Internet]. 2015 Feb 17 [cited 2019 Jun 3];45(2):109–27. Available from: http://www.ncbi.nlm.nih.gov/pubmed/24785737

4. Schandené L, Cogan E, Crusiaux A, Goldman M. Interferon-α Upregulates Both Interleukin-10 and Interferon-γ Production by Human CD4+ T Cells. Blood. 1997;89(3):1110–1.

5. Hervas-Stubbs S, Perez-Gracia JL, Rouzaut A, Sanmamed MF, Le Bon A, Melero I. Direct Effects of Type I Interferons on Cells of the Immune System. Clin Cancer Res [Internet]. 2011 May 1 [cited 2019 Jun 3];17(9):2619–27. Available from: http://www.ncbi.nlm.nih.gov/pubmed/21372217

6. Pestka S, Krause CD, Walter MR. Interferons, interferon-like cytokines, and their receptors. Immunol Rev [Internet]. 2004 Dec [cited 2019 Jun 3];202(1):8–32. Available from: http://www.ncbi.nlm.nih.gov/pubmed/15546383

7. Radwanski E, Perentesis G, Jacobs S, Oden E, Affrime M, Symchowicz S, et al. Pharmacokinetics of interferon alpha-2b in healthy volunteers. J Clin Pharmacol [Internet]. 1987 [cited 2019 Jun 5];27(5):432–5. Available from: http://www.ncbi.nlm.nih.gov/pubmed/3693589

8. Boulestin A, Kamar N, Sandres-Sauné K, Alric L, Vinel J-P, Rostaing L, et al. Pegylation of IFN-alpha and antiviral activity. J Interferon Cytokine Res [Internet]. 2006 Dec [cited 2019 Jun 3];26(12):849–53. Available from: http://www.liebertpub.com/doi/10.1089/jir.2006.26.849

9. Akash MSH, Rehman K, Chen S. Polymeric-based particulate systems for delivery of therapeutic proteins. Pharm Dev Technol [Internet]. 2016;21(3):367–78. Available from: http://dx.doi.org/10.3109/10837450.2014.999785

10. Hamid Akash MS, Rehman K, Chen S. Natural and synthetic polymers as drug carriers for delivery of therapeutic proteins. Polym Rev. 2015;55(3):371–406.

11. Mukhopadhyay P, Kundu PP. Chitosan-graft-PAMAM–alginate core–shell nanoparticles: a safe and promising oral insulin carrier in an animal model. RSC Adv [Internet]. 2015 Nov 2 [cited 2019 Sep 20];5(114):93995–4007. Available from: http://xlink.rsc.org/?DOI=C5RA17729D

12. Sheng J, He H, Han L, Qin J, Chen S, Ru G, et al. Enhancing insulin oral absorption by using mucoadhesive nanoparticles loaded with LMWP-linked insulin conjugates. J Control Release [Internet]. 2016 Jul 10 [cited 2019 Sep 20];233:181–90. Available from: https://linkinghub.elsevier.com/retrieve/pii/S0168365916302784

13. Zhang Y, Wei W, Lv P, Wang L, Ma G. Preparation and evaluation of alginate-chitosan microspheres for oral delivery of insulin. Eur J Pharm Biopharm [Internet]. 2011 Jan [cited 2019 Sep 20];77(1):11–9. Available from: https://linkinghub.elsevier.com/retrieve/pii/S0939641110002596

14. Sonaje K, Lin Y-H, Juang J-H, Wey S-P, Chen C-T, Sung H-W. In vivo evaluation of safety and efficacy of self-assembled nanoparticles for oral insulin delivery. Biomaterials [Internet]. 2009 Apr [cited 2019 Sep 20];30(12):2329–39. Available from: https://linkinghub.elsevier.com/retrieve/pii/S0142961208010661

15. Cánepa C, Imperiale J, Berini C, Lewicki M, Sosnik A, Biglione M. Development of a Drug Delivery System Based on Chitosan Nanoparticles for Oral Administration of Interferon-α. Biomacromolecules. 2017;18:3302–9.

16. Hirai A, Odani H, Nakajima A. Determination of degree of deacetylation of chitosan by 1H NMR spectroscopy. Polym Bull. 1991;26:87–94.

17. Schlachet I, Trousil J, Rak D, Knudsen KD, Pavlova E, Nyström B, et al. Chitosan-graft-poly(methyl methacrylate) amphiphilic nanoparticles: Self-association and physicochemical characterization. Carbohydr Polym [Internet]. 2019 May 15 [cited 2019 Jul 24];212:412–20. Available from: http://www.ncbi.nlm.nih.gov/pubmed/30832875

18. Chang F-C, Tsao C-T, Lin A, Zhang M, Levengood SL, Zhang M. PEG-chitosan hydrogel with tunable stiffness for study of drug response of breast cancer cells. Polymers (Basel) [Internet]. 2016 Mar 26 [cited 2019 Jun 3];8(4):112. Available from: http://www.mdpi.com/2073-4360/8/4/112

19. Sarmento B, Mazzaglia D, Bonferoni MC, Neto AP, do Céu Monteiro M, Seabra V. Effect of chitosan coating in overcoming the phagocytosis of insulin loaded solid lipid nanoparticles by mononuclear phagocyte system. Carbohydr Polym [Internet]. 2011 Mar 17 [cited 2019 Jun 3];84(3):919–25. Available from: https://www.sciencedirect.com/science/article/pii/S0144861710010283

20. Xu Q, Ensign LM, Boylan NJ, Schön A, Gong X, Yang J-C, et al. Impact of Surface Polyethylene Glycol (PEG) Density on Biodegradable Nanoparticle Transport in Mucus *ex Vivo* and Distribution *in Vivo*. ACS Nano [Internet]. 2015 Sep 22 [cited 2019 Jun 4];9(9):9217–27. Available from: http://pubs.acs.org/doi/10.1021/acsnano.5b03876

21. A Natural Source of Chitosan | ChitoClear | Primex [Internet]. [cited 2019 Jun 3]. Available from: http://www.primex.is/products-services/chitoclear/

22. Noi I, Schlachet I, Kumarasamy M, Sosnik A. Permeability of Novel Chitosan-g-poly (Methyl Methacrylate) Amphiphilic Nanoparticles in a Model of Small Intestine in Vitro. Polymers (Basel) [Internet]. 2018 Apr 18 [cited 2019 Jun 6];10:478. Available from: https://www.preprints.org/manuscript/201804.0245/v1

23. Lea T. Caco-2 Cell Line. In: The Impact of Food Bioactives on Health [Internet]. Cham: Springer International Publishing; 2015 [cited 2019 Jun 6]. p. 103–11. Available from: http://link.springer.com/10.1007/978-3-319-16104-4_10

24. Yee S. In vitro permeability across Caco-2 cells (colonic) can predict in vivo (small intestinal) absorption in man--fact or myth. Pharm Res [Internet]. 1997 Jun [cited 2019 Jun 3];14(6):763–6. Available from: http://www.ncbi.nlm.nih.gov/pubmed/9210194

25. Cummins JM, Beilharz MW, Krakowka S. Oral use of interferon. J Interferon Cytokine Res [Internet]. 1999 Aug [cited 2019 Jun 3];19(8):853–7. Available from: http://www.liebertpub.com/doi/10.1089/107999099313352

26. Coppi G, Sala N, Bondi M, Sergi S, Iannuccelli V. Ex-vivo evaluation of alginate microparticles for Polymyxin B oral administration. J Drug Target [Internet]. 2006 Jan 8 [cited 2019 Jun 3];14(9):599–606. Available from: http://www.tandfonline.com/doi/full/10.1080/10611860600864182

27. Chatelut E, Rostaing L, Grégoire N, Payen JL, Pujol A, Izopet J, et al. A pharmacokinetic model for alpha interferon administered subcutaneously. Br J Clin Pharmacol [Internet]. 1999 Apr [cited 2019 Jul 24];47(4):365–71. Available from: http://doi.wiley.com/10.1046/j.1365-2125.1999.00912.x